Supplemental Data

Structure of the Pho85-Pho80 CDK-Cyclin

Complex of the Phosphate-Responsive

Signal Transduction Pathway

Kexin Huang, Ian Ferrin-O'Connell, Wei Zhang, Gordon A. Leonard, Erin K. O'Shea, and Florante A. Quiocho

Supplemental Experimental Procedures

Bacterial Expression and Purification of Pho85-Pho80

Co-expression of Pho85-His$_6$ and Pho80 in *E. coli* essentially follows the

published procedure (Jeffery et al., 2001). Briefly, the full length Pho85-His$_6$ and

Pho80 were co-expressed in BL21 DE3 (Novagen) by adding isopropyl-β-D-

thiogalactopyranoside (IPTG) to final concentration of 200 μM at 24°C after the

cells are grown to A$_{595}$ of 0.4 – 0.6. Following cell lysis by microfluidizer

processor (Microfluidics), the His$_6$-Pho85-Pho80 was purified through Ni

Sepharose High Performance and HiTrap Heparin High Performance columns

(Amersham Biosciences). Similar procedure was used to express and purify the

seleno-methionine variant of Pho85-Pho80 using *E. coli* B834 methionine

auxotroph strain (Novagen). The purified native and Se-Met His$_6$-Pho85-Pho80

are essentially monodisperse as judged by dynamic light scattering

measurement.

Crystallization and Diffraction Data Collection

Long needle-shaped crystals of the complex were grown in hanging drops at 10°C by mixing 3 volumes of the concentrated Pho85-Pho80 and 2 volumes of the reservoir solutions of 9 to 12% PEG 10K, 10% glycerol, 0.2 – 0.25 M strontium chloride (SrCl$_2$), 10 mM Tris (2-carboxyethyl) phosphine (TCEP) and 0.1 M 2-morpholinoethanesulfonic acid (MES), pH6.5.   Crystals of the complex of Pho85-Pho80 in the presence of ATP-γ-S (Sigma) were obtained by microseeding. The crystals were cryo-protected by coating with paratone-N oil before flash-freezing in liquid nitrogen.

Both ligand-free and ATP-γ-S-bound crystals belong to the same space group and have very similar unit cell dimensions (Table 1). Based on the Matthews coefficient analysis (Kantardjieff and Rupp, 2003; Matthews, 1968), the number of Pho85-Pho80 heterodimer molecules in the asymmetric unit could not be determined with certainty; assuming 2, 3 and 4 heterodimers in the asymmetric unit, the calculated solvent content are approximately 75, 62 and 50%, respectively.

Determination of the Crystal Structure of Pho85-Pho80

Although Pho85 shares 55% identity with CDK2, the use of molecular replacement technique to obtain initial phases, with the main chain of the crystal structure of CDK2 (PDB code: 1QMZ) as the search model, was not successful. Therefore, a single-wavelength anomalous dispersion (SAD) data set (Table 1) was collected at the microfocus beamline ID29, ESRF, Grenoble, France and

processed and analyzed using MOSFLM (Leslie, 1992). The Pho85-Pho80 heterodimer has a total of twelve methionines (nine in Pho85 and three in Pho80), including the initiator M1 residues in both proteins. Excluding the two N-termini methionines, most (~80%) of the expected selenomethionine (or Se) sites resides in Pho85. Twelve Se sites were identified in SOLVE (Terwilliger and Berendzen, 1999) using the SAD data at the peak wavelength. These sites were refined in SHARP (La Fortelle and Bricogne, 1997) using the data between 30-3.5 Å. However, the overall experimental figure of merit was quite poor (~0.3), and the SAD-phased electron density map was not good enough to discern useful structural features and intermolecular boundaries.

We then used pattern matching in attempts to assess the correctness and relationship of the initial twelve sites and the existence of non-crystallographic symmetry (NCS). After measuring the distances between every two Se sites, we could identify two sets of three Se sites with nearly identical triangular geometries. Noting the locations of the residues in the CDK2 crystal structure (PDB code: 1QMZ) that align with the eight internal methionines of the Pho85 sequence (two being identical to CDK2 sequence), we could also find a set of three methionine positions in the CDK2 structure that match with either of the two sets of three Se sites identified in the pattern matching. Taken together, the results indicate that the two sets of three Se sites are related by a NCS and that there are two heterodimers in the asymmetric unit. Indeed, the NCS matrix was found by FINDNCS (Lu, 1999). A SAD phased (based on the 12 seleno sites), two-fold NCS averaged and solvent flattened (75% solvent) electron density map at 3.5 Å showed considerable improvement and was very encouraging.

Molecular boundaries could be made out. The Cα trace of the crystal structure of CDK2, which has a significant sequence identity and similarity to Pho85, could be fitted reasonably well as an entire rigid body to the Pho85 density in the two heterodimers. More importantly, we could confirm not only the positions of the initial twelve Se sites but also found seven more sites from SHELXD (Schneider and Sheldrick, 2002) and SnB (Weeks and Miller, 1999). The nineteen total sites (ten in one heterodimer complex and nine in the other complex) were refined in SHARP and used to calculate another 2-fold averaged and solvent flattened map (figure of merit of 0.85). The densities of a significant number of side chains were revealed. Model building was done with the programs COOT (Emsley and Cowtan, 2004) and O (Jones et al., 1991). The model was refined against the native dataset, collected at the APS ID19 beamline, with CNS (Brunger et al., 1998) and CCP4 (CCP4, 1994) package.

Site-Directed Mutagenesis and Kinase Assays

      Fusion PCR was used to generate Pho80 mutants, F138A with the following primers:

5'-AAAGGCTTATGTGATTCG<u>GCC</u>TCAACAAACGCCCATTAT-3' and

5'-ATAATGGGCGTTTGTTGA<u>GGC</u>CGAATCACATAAGCCTTT-3' and F138E with the following primers:

5'-AAAGGCTTATGTGATTCG<u>CAA</u>TCAACAAACGCCCATTAT-3' and

5'-ATAATGGGCGTTTGTTGA<u>TTG</u>CGAATCACATAAGCCTTT-3'. In both cases, the underlined sequence represents the mutated codon that was inserted into the PCR product. Subsequently the following primers were utilized for both mutants:

5'-TCACAACATATGGAAAGCACATCAGGA-3' and

5'-CATCAAGGATCCTTAATCTGGCTTTGATCG-3', which are complimentary to

nucleotides +1 to +18 and +865 to +882 of the *PHO80* gene, respectively. All

PCR reactions were carried out with $Vent_R$ polymerase according to the

manufacturer's instructions (New England Biolabs). After cutting the PCR product

into the pSBET-a vector (Schenk et al., 1995), the presence of the appropriate

mutation was verified by sequencing.

Quick change mutagenesis was performed on EB1285 using the Quick

Change II kit (Stratagene) to generate the Pho80 distal mutants with the following

primer pairs:

5'-CAAAAGTAATTCTGCCCGCTGATTTTAATAAATATTCTAGAACTGA-

CCTAGT-3' and 5'-

ACTAGGTCAGTTCTAGAATATTTATTAAAATCAGCGGGCA-GAATTACTTTTG-

3' for C30Y, 5'-CTAGAACTGACCTAGTGGTGTTCATA-TCACGAATGTTAGTA-

3' and 5'-TACTAACATTCGTGATATGAACACCACTAGG-TCAGTTCTAG-3' for

L38F, 5'-CCTAGTGGTGCTCATATCACAAATGTTAGTAT-CGCTGATAG-3' and

5'-CTATCAGCGATACTAACATTTGTGATATGAGCACCA-CTAGG-3' for R41Q,

and 5'-GAATAGTTCAGCTGGTGGATTCCTTTAACGCTT-CACC-3' and 5'-

GGTGAAGCGTTAAAGGAATCCACCAGCTGAACTATTC-3' for G229D. In each

case, the underlined sequence represents the nucleotide(s) that was modified.

These EB1285 based vectors were then cut with BamHI and NdeI (New England

Biolabs) and the Pho80 fragment was ligated into a pSBET-a vector (Schenk et

al., 1995). Following ligation, all mutations were verified by sequencing. Co-

expression of Pho85-His_6 and the Pho80 mutants in *E. coli,* and their

purifications, essentially follows the published procedure (Jeffery et al., 2001). The Pho80 distal site mutants were further purified using an isocratic elution from a HiLoad 16/60 75 pg gel filtration column (GE Healthcare), and the 1:1 stoichiometry of Pho85-His$_6$:Pho80 was confirmed via Safe Blue staining (Invitrogen).

The kinase assays were carried out following published procedure (Jeffery et al., 2001). The Pho4 substrate was purified according to a published procedure (Jeffery et al., 2001). The peptides used in kinase assays (identified as SPVI and SPVA) were made by Biosynthesis, Inc. and Bethyl Laboratories, Inc. respectively. SPVI, which corresponds to the SP6 phosphorylation site of Pho4 (O'Neill et al., 1996), has the sequence 213SAEGVVVASE**SPVI**APHGSTHARSY237, where the consensus sequence (**SPVI**) is in bold. SPVA, the non-specific substrate, is identical to the SPVI peptide substrate but with the I residue at the +3 position of the consensus sequence changed to A. For analysis of SPVI phosphorylation by the Pho80 distal site mutants, the dried p81 discs were exposed to a storage phosphor screen and imaged using the Typhoon Trio system (GE Healthcare).

Identification of a Shorter Segment of the 80 Residue Fragment of Pho81 that Binds Pho85-Pho80

We sought to determine whether there is a shorter segment of the 80-residue (644 to 723) segment/domain of Pho81, initially shown to be necessary for the inhibition of the kinase activity (Huang et al., 2001), that will bind Pho85-Pho80. Eight different truncation constructs (shown in Figure S4) of the 80-residue
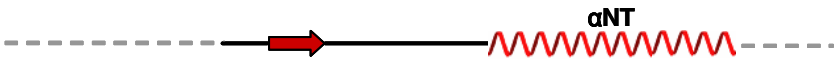
domain were cloned into the pTYB11 expression vector of the IMPACT T7 System (New England Biolabs) as an intein fused to a chitin binding domain (CBD). A pull down assay was used to determine the interaction between each truncation mutant and Pho85-Pho80. About 50 µl of the chitin beads was mixed with 1 ml cell lysate of each truncation mutant–INTEIN-CBD. The beads were then centrifuged for 30 seconds at 1,000g, and the pellet suspended in 1 ml of 500 mM NaCl, 5% glycerol and 20 mM Tris, pH 8.0; this procedure was repeated five times to remove protein contaminants bound non-specifically to the chitin beads. The beads were then mixed with excess amount of purified Pho85-Pho80 and incubated for one hour. After subjecting the beads to extensive washing as described above, a sample was chromatographed on a SDS gel electrophoresis and the gel stained with Coomasie Blue. As shown in Figure S4, a shorter segment of the primary sequence of Pho81, which comprises of residues 665 to 701, can bind Pho85-Pho80. The fact that Pho85-Pho80 remained bound to the segment despite extensive washing of the beads indicates a tight complex. The 37-residue segment includes residues 690 to 695 and 699 to 701 which when mutated in Pho81 caused significant defects in inducing Pho5 expression (Huang et al., 2001). Interestingly, RXL motif is not present in the shorter segment that binds Pho85-Pho80. Although there is one putative RXL motif at residue 647 to 649 (RPL) of the 80-residue domain, the three truncation mutants (644-652, 644-658 and 644-664) which harbor the RXL motif do not bind Pho85-Pho80 (Figure S4).

Table S1. Substrates of Pho85-Pcl Complexes and the D Loop Sequences of the Pho80/Pcl Subunits

Cyclin subunit	Substrate			Sequence of D-loops in Pcls[b]
	Name	Sequence[a]	Reference	
Pho80	Pho4	SPXI/L (5 sites)	(O'Neill et al., 1996)	DS<u>F</u>SF
"	Rim15 kinase	T^{1075}PPL	(Reinders et al., 1998)	DS<u>F</u>SF
Pcl1	Sic1	T^{5}PPR	(Nishizawa et al., 1998)	DS<u>S</u>PL
Pcl2	Rvs167	S^{299}PVS, S^{379}PPL	(Friesen et al., 2003)	DS<u>S</u>PL
Pcl5	Gcn4	T^{105}PMF, T^{165}PVL	(Meimoun et al., 2000; Shemer et al., 2002)	DN<u>T</u>YS
Pcl6/7	Gcl8	T^{118}PYQ	(Tan et al., 2003)	DF<u>F</u>YS
Pcl10	Gsy2	S^{654}PRD	(Wilson et al., 1999)	DF<u>V</u>HS

[a]Sequence of the peptide segment containing the phosphorylatable S or T residue.
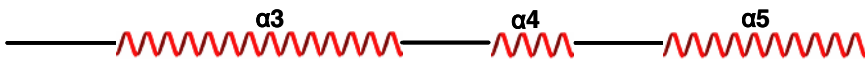
[b]Based on amino sequence alignment of the Pho80/Pcls (Supplementary Figure S1). The first residue (D), which is involved in a functional salt link with Pho85 R132 (see Text), is invariant in all ten cyclins. The third residue (F138) of the Pho80 D-loop is potentially involved in recognizing I/L at position +3 of the phosphorylatable sites on Pho4 (see Text).

αNT

```
Pho80  ---MESTSGERSENIHEDQGIPKVILPADFNKCSRTDLVVLISRMLVSLIAINENSATKK  57
pcl1   ------------------------------------------------------------
pcl2   --------------------------------------------------VSKEMVQYLASTTAS  29
pcl5   ------------------------------------------------------------
pcl6   ------------------------------------------------------------
pcl7   EAKTHSLDEETNEQTDVKILNIADFPTDELILMISALLNRIITANDETTDVSQQVSDETE  140
pcl8   ---------------ESIPKIPELSDDEALSKFRENIELILQLSKKINDNANTLAISSE  348
pcl9   ------------------------------------------------------------
pcl10  ---------------PVDVEVPHISVDEALANFKETIELLLKLSG--NRKCTGFNTRVE  293
Clg1   ------------------------------------------------------------
```

α1   α2

```
Pho80  SDDQITLTRYHSKIPPNISIFNYFIRLTKFSSLEHCVLMTSLYYIDLLQT----------  107
pcl1   -----------------SLMTFITRLVRYTNVYTPTLLTAACYLNKLKR----------  85
pcl2   IIKIKKTNSMIDIALPAPPLTKFINRLIKHSNVQTPTLMATSVYLAKLRS----------  79
pcl5   -------------------ILKFLNEVLKRSKCSKENAVLATFYFQKIHQSR------GV  114
pcl6   ---------------QIGLDQYFQRIQKYCPTTNDVFLSLLVYFDRISKR---------  264
pcl7   DELLTPILAFYGKNVPEIAVVQYLERIQKYCPTTNDIFLSLLVYFDRISKNYGHSSERNG  200
pcl8   DP--QKFVNFVMKNPPSLSFRDFIDRIQNKCMFGAVVYLGATYLLQLVFLTR---DEMDG  403
pcl9   ----------------PPDLSIFIKNVVIQSNVQTPTLMATSVYLNKLKS----------  79
pcl10  K---KEYSNFYMKSKPTLSSADFLKRIQDKCEYQPTVYLVATFLIDTLFLTR---DGNN-  346
Clg1   ---------------------YINKLSNGIHSIGGNSIN-IIYQN--------------  214
```

α3   α4   α5

```
Pho80  -VYPDFTLNSLTAHRFLLTATTVATKGLCDSFSTNAHYAKVGG--VRCHELNILENDFLK  164
pcl1   ILPRDATGLPSTIHRIFLACLILSAKFHNDSSPLNKHWARYTDGLFTLEDINLMERQLLQ  145
pcl2   IIPSNVYGIETTRHRIFLGCLILAAKTLNDSSPLNKHWAEYTDGLLILREVNTIERELLE  139
pcl5   RDESSLPEFSHCSRRIFLCCLILSHKFLNDNTYSMKNWQIISG--LHAKDLSLMERWCLG  172
pcl6   CNSQMFVMDSHNIHRLIIAGITVSTKFLSDFFYSNSRYSRVGG--ISLQELNHLELQFLV  382
pcl7   CAKQLFVMDSGNIHRLLITGVTICTKFLSDFFYSNSRYAKVGG--ISLQELNHLELQFLI  258
pcl8   PIKLKAKLQEDQAHRIIISTIRIATKLLEDFVHSQNYICKVFG--ISKRLLTKLEISFMA  461
pcl9   VIPKNVYGINTTRHRIFLGCLILAAKTLNDSSPWNKHWTTYEGLLRIREVNTIERELLE  139
pcl10  ILQLKLNLQEKEVHRMIIAAVRLSTKLLEDFVHSHEYFSKVCG--ISKRLLTKLEVSLLI  404
Clg1   ----------------TMIAFILANKFNDDKTFTNNSWSQATG--ILINVINDFERQWLR  256
                               ★
```

```
                αCT1                                              αCT2
         _____  MMM _____    - - - -    _____   MMM

Pho80    RVNYRIIPRDHNITLCSIEQKQKKFVIDKNALGSLDLDSYSYVNRPKSGYNVLDKYYRRI   224
pcl1     LLNW--------------------------------------------------------   149
pcl2     YFDWDVTISTDDLITC---------------------------------------------   155
pcl5     KLNYELAIPYDE-------------------------------------------------   184
pcl6     LCDFELLI----------------------------------------------------   390
pcl7     LCDFKLLVSVEEMQK----------------------------------------------   273
pcl8     SVNF--------------------------------------------------------   465
pcl9     YLNWDV------------------------------------------------------   145
pcl10    CVCN--------------------------------------------------------   408
Clg1     IFNW--------------------------------------------------------   260


              MMM _____   ___▶___   - - - - - - - - - - - -

Pho80    VQLVGSFNASPDKSRKVDYVLPPNIDIVSESGSQTTQLKGSSSPNSHSSQKRYSEAKDAH   284
pcl1     ------------------------------------------------------------
pcl2     ------------------------------------------------------------
pcl5     ------------------------------------------------------------
pcl6     ------------------------------------------------------------
pcl7     ------------------------------------------------------------
pcl8     ------------------------------------------------------------
pcl9     ------------------------------------------------------------
pcl10    ------------------------------------------------------------
Clg1     ------------------------------------------------------------


              - - - - - - -

Pho80    IYNKRSKPDY
pcl1     ----------
pcl2     ---------M
pcl5     ----------
pcl6     ----------
pcl7     ---------F
pcl8     ---------F
pcl9     ----------
pcl10    ---------F
Clg1     ----------
```
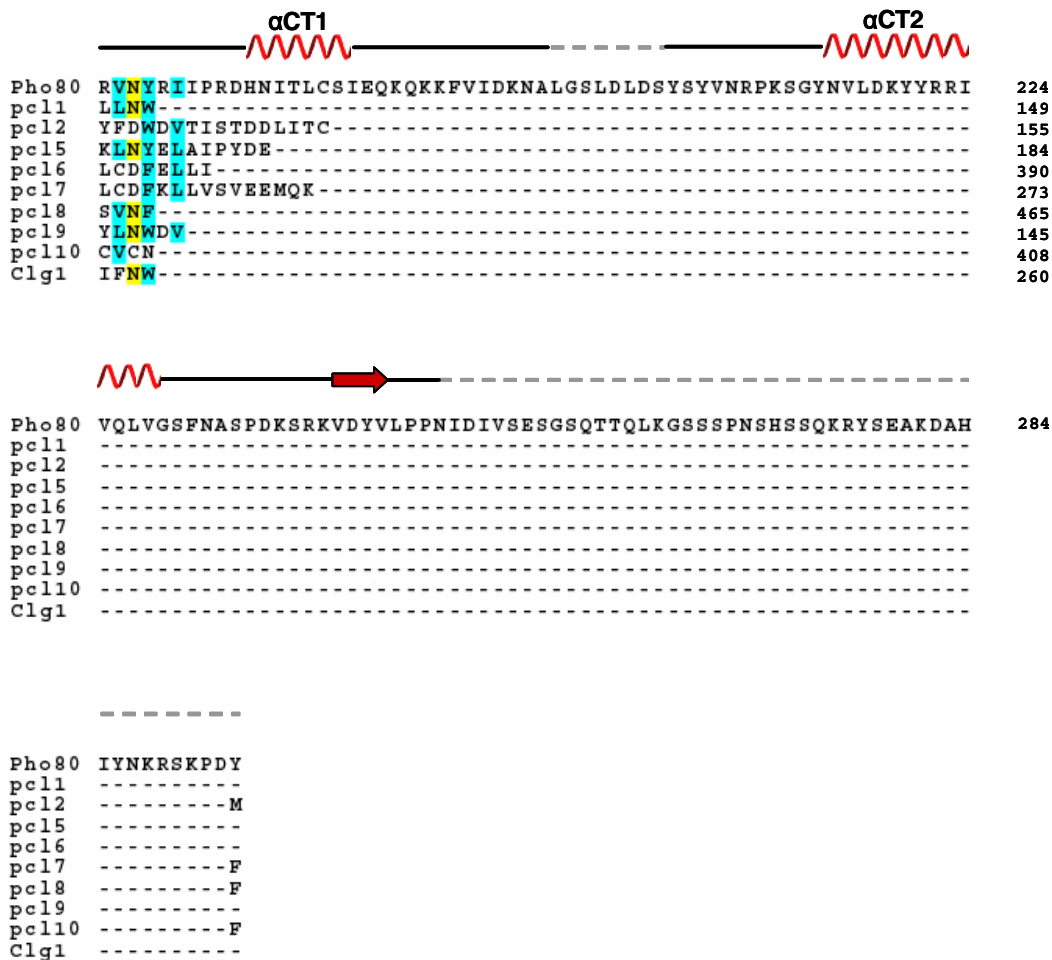
Figure S1. Amino Acid Sequence Alignment of Pho80 and the Other Nine

***P*ho85 *Cycl*ins (Pcls)**

The alignment was done using Clustal W program and colored by the Boxshade

Program. The α helices, loops and the two short strands of one β sheet as they

occur in the Pho80 structure are placed above the alignment. The residues that

are completely invariant, identical and similar are highlighted in green, yellow and

cyan backgrounds, respectively. The numbers on the right hand side correspond

to the amino acid positions in the primary sequences. The star identifies the position of an invariant aspartic acid residue (D136 in Pho80). Dashed lines indicate disordered segments in the structure, consisting of an eight-residue segment in the middle of the αNT-α1 loop and a five-residue segment in the middle of the αCT1-αCT2 loop (see also Figure 1A in the main paper). The Pcl6 sequence (residues 230 to 390) could be aligned only after excluding the 70-residue segment from 268 to 327. The excluded segment, which is predicted to be between α2 and α3, is considerably longer than the corresponding segments in Pho80 and other Pcls.
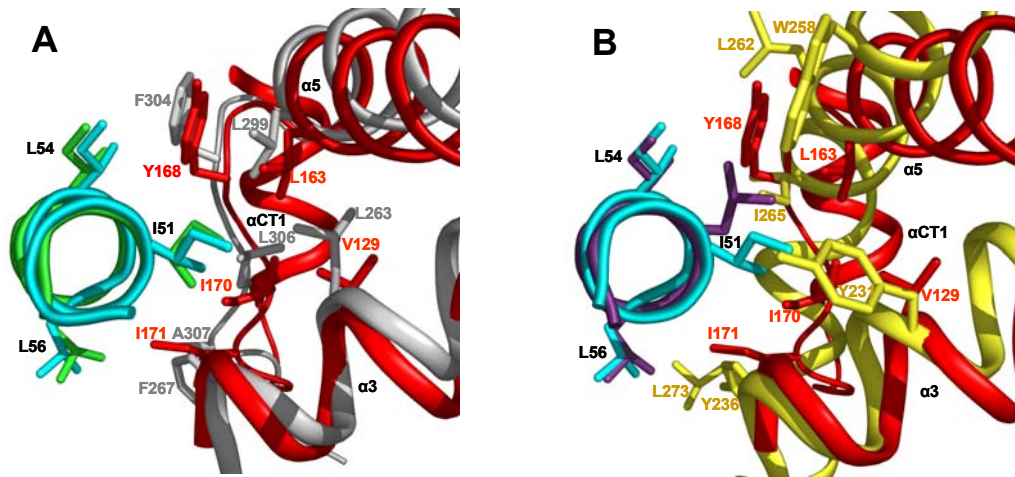
Figure S2. Hydrophobic Interactions of the Aliphatic Residues on the PSTAIRE/PSSALRE Helices of Pho85, CDK2, and CDK5 with Residues of Their Respective Cyclins

The PSTAIRE in Pho85 and CDK2 are shown in cyan and green, respectively, and the PSSALRE in CDK5 is shown in purple. The cyclins are depicted in red for Pho80, grey for cyclin A and yellow for p25. Residue identifications (black color for the PSTAIRE helix and red for the cyclin) are for only the Pho85-Pho80 complex. The residues of cyclin A and p25 are shown in grey and orange, respectively. The overlaps in panels A and B were obtained following superposition of the kinase subunit structures. The three PSTAIRE/PSSALRE helices adopt virtually identical position. The hydrophobic interactions between the aliphatic residues on the PSTAIRE/PSSALRE and cyclin residues are summarized below. The locations of the residues on the cyclins are in parenthesis.

Pho85	Pho80	CDK2	Cyclin A	CDK5	P25
I51	V129 (α3) L163 (α5) I170 (loop after α5)	I49	L263 (α3) L299 (α5) L306 (loop after α5)	L49	Y231(α3) W258 (α5) I265 (α5)
I54	Y168 (loop after α5)	I52	F304 (loop after α5)	I52	L262 (α5)
L56	I171 (loop after α5)	L54	A307 (loop after α5) F267 (α3)	L54	Y236 (α3) L273 (αCT1)

(A) Overlap of the Pho85 and CDK2 PSTAIRE helices and parts of Pho80 and cyclin A. Both α3 and α5 in Pho80 and cyclin A adopt roughly a similar position. αCT1 in Pho80 has no counterpart in cyclin A. Note that the locations of the three aliphatic residues on the PSTAIREs involved in the interactions with the cyclins are almost identical (summarized in the table above). Moreover, the residues on the cyclins involved in the interactions originate from identical segments (see table).

(B) Overlap of Pho85-Pho80 and CDK5-p25. In contrast to that shown in panel A, the α5 helices of Pho80 and p25 barely overlap (see also Figure S3). Moreover, in p25, residues from almost entirely the C-termini of helices α3 and α5 and the N-terminus of αCT1 make interactions with the large aliphatic side chains on PSSALRE. This difference is attributed mainly to the differences in the geometries of α5 and its neighboring helices between p25 and Pho80 or cyclin A (further discussed in Figure S3 legend). Among the three different aliphatic side chains on PSTAIRE or PSSALRE helix, only L49 of CDK5 fails to overlap with the corresponding I51 of Pho85 or I49 of CDK2. This difference may be attributed to the interactions in p25 of L49 with two bulkier aromatic residues (Y231 and W258), thereby possibly nudging L49 farther to one side, as

compared with the interactions of I51 of Pho85 or I49 of CDK2 with only aliphatic side chains.
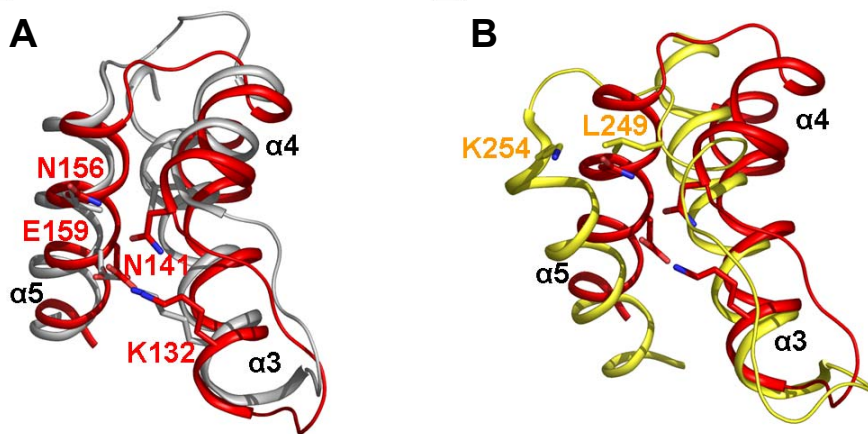

Figure S3. The Relationship of the α5 Helices with α3 and α4 of Pho80 or Cyclin A and with α3 of p25

The color schemes for the helices and residue numbers are identical to those described in Figure S2. The overlaps shown in panels A and B were obtained following superposition of the kinase subunit structures.

(A) The geometries of the helices α3, α4 and α5 in Pho80 (red) and cyclin A (grey). Note the similarities of the geometries in the two complexes, notably all three helices in both cyclins adopting quite similar positions. Moreover, as shown in Figure 1A in main text, the α5 helices in Pho80 and cyclin A lie nearly parallel to the PSTAIRE helices. A salt link and a hydrogen bond or hydrophobic interaction contribute to maintaining the close packing of α5 to the cyclin box in

both Pho80 and cyclin A. The salt link (lower pair) in Pho80, between E159 on α5 and K132 on α3, is equivalent to that in cyclin A, between E295 on α5 and K266 on α3 (data not shown). A hydrogen bond is also formed in Pho80 between N156 on α5 and N141 on α4 (the upper pair). In place of the hydrogen bond, a hydrophobic interaction is formed in cyclin A, between L292 on α5 and V275 on α4 (data not shown).

(B) The relationship between α5 and α3 in Pho80 (red) and p25 (yellow). Despite the claim of the presence of α4 helix in p25 (Tarricone et al., 2001), PDB analysis indicates clearly that it is missing (see also Figure 1B in the main text). In contrast to the similar geometry shown in panel A for Pho80 and cyclin A, in p25, the position of α5 differs from that in Pho80 or cyclin A. The p25 α5 helix is farther away from the rest of the cyclin box helix bundle. The angle between the axes of α5 helices in p25 and Pho80 is 27°. Moreover, whereas the α5 helices in Pho80 and cyclin A lie parallel to the PSTAIRE, the α5 helix in p25 is rotated at an angle of about ~25° with respect to PSSALRE (Figure 1B in the main text). The reasons for the geometrical difference are not clear, but one possibility is the absence in p25 of the two stabilizing interactions between helices α3 and α5 in Pho80 and cyclin A (panel A).   Additionally, the juxtaposition and noncomplementarity between L249, which resides on the long loop following α3 and roughly assumes a similar position to that of N156 on α5 of Pho80, and K254 on α5 could be another determinant in attaining the final geometry in p25. Since α3 α4 and α5 of the cyclin box in Pho85 and p25 are engaged extensively in the interaction with the cognate kinase subunits, the differences in the geometries of these helices may account for the plasticity of the CDK-cyclin interfaces. The

difference in the position of α5 in p25 as compared to that in cyclin A (or now Pho80) has been attributed to be the consequence of the tight packing of αNT against α1, α2, and the last portion of α7, the equivalent of αCT2 (Tarricone et al., 2001). A problem of this explanation is that the packing geometry of the four helices in p25 is not too different from that in Pho80 (see Figure 1B in the main text).
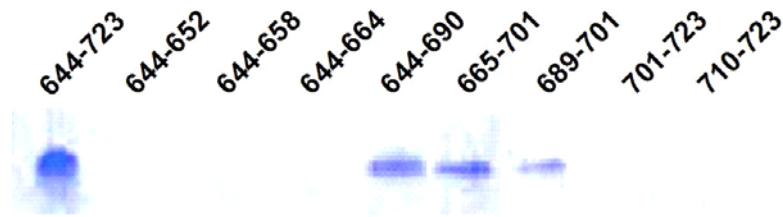
Figure S4. Identification of a Shorter Segment of the 80 Residue Fragment of Pho81 that Binds Pho85-Pho80

Binding was demonstrated by pull down assays with the segment-INTEIN-CBD bound to chitin beads serving as a bait to retrieve Pho85-Pho80. The stronger intensity of the Pho85-Pho80 band pulled down by the 80-residue fragment (644-723) is probably a reflection of a better expression of the 80-residue-INTEIN-CBD construct and a much larger fragment.

Supplemental References

Brunger, A. T., Adams, P. D., Clore, G. M., DeLano, W. L., Gros, P., Grosse-Kunstleve, R. W., Jiang, J. S., Kuszewski, J., Nilges, M., Pannu, N. S.*, et al.* (1998). Crystallography & NMR system: A new software suite for macromolecular structure determination. Acta Crystallogr *D54*, 905-921.

CCP4 (1994). Collaborative Computational Project No.4. The CCP4 programs for protein crystallography. Acta Crystallogr *D50*, 760-763.

Emsley, P., and Cowtan, K. (2004). Coot: model-building tools for molecular graphics. Acta Crystallogr *D60*, 2126-2132.

Friesen, H., Murphy, K., Breitkreutz, A., Tyers, M., and Andrews, B. (2003). Regulation of the yeast amphiphysin homologue Rvs167p by phosphorylation. Mol Biol Cell *14*, 3027-3040.

Huang, S., Jeffery, D. A., Anthony, M. D., and O'Shea, E. K. (2001). Functional analysis of the cyclin-dependent kinase inhibitor Pho81 identifies a novel inhibitory domain. Mol Cell Biol *21*, 6695-6705.

Jeffery, D. A., Springer, M., King, D. S., and O'Shea, E. K. (2001). Multi-site phosphorylation of Pho4 by the cyclin-CDK Pho80-Pho85 is semi-processive with site preference. J Mol Biol *306*, 997-1010.

Jones, T. A., Zou, J. Y., Cowan, S. W., and Kjeldgaard (1991). Improved methods for building protein models in electron density maps and the location of errors in these models. Acta Crystallogr *A47*, 110-119.

Kantardjieff, K. A., and Rupp, B. (2003). Matthews coefficient probabilities: Improved estimates for unit cell contents of proteins, DNA, and protein-nucleic acid complex crystals. Protein Sci *12*, 1865-1871.

La Fortelle, E. D., and Bricogne, G. (1997). SHARP program for statistical heavy-atom refinement. Methods Enzymol *276*, 472-494.

Leslie, A. G. W. (1992). Recent changes to the MOSFLM package for processing film and image plate data. Joint CCP4 ESF-EACBM Newsl Protein Crystallogr *26*.

Lu, G. (1999). FINDNCS: a program to detect non-crystallographic symmetries in protein crystals from heavy-atom sites. J Appl Crystallogr *32*, 365-368.

Matthews, B. W. (1968). Solvent content of protein crystals. J Mol Biol *33*, 491-497.

Meimoun, A., Holtzman, T., Weissman, Z., McBride, H. J., Stillman, D. J., Fink, G. R., and Kornitzer, D. (2000). Degradation of the transcription factor Gcn4 requires the kinase Pho85 and the SCF(CDC4) ubiquitin-ligase complex. Mol Biol Cell *11*, 915-927.

Nishizawa, M., Kawasumi, M., Fujino, M., and Toh-e, A. (1998). Phosphorylation of Sic1, a cyclin-dependent kinase (Cdk) inhibitor, by Cdk including Pho85 kinase is required for its prompt degradation. Mol Biol Cell *9*, 2393-2405.

O'Neill, E. M., Kaffman, A., Jolly, E. R., and O'Shea, E. K. (1996). Regulation of PHO4 nuclear localization by the PHO80-PHO85 cyclin-CDK complex. Science *271*, 209-212.

Reinders, A., Burckert, N., Boller, T., Wiemken, A., and De Virgilio, C. (1998). Saccharomyces cerevisiae cAMP-dependent protein kinase controls entry into stationary phase through the Rim15p protein kinase. Genes Dev *12*, 2943-2955.

Schenk, P. M., Baumann, S., Mattes, R., and Steinbiss, H. H. (1995). Improved high-level expression system for eukaryotic genes in Escherichia coli using T7 RNA polymerase and rare ArgtRNAs. Biotechniques *19*, 196-198, 200.

Schneider, T. R., and Sheldrick, G. M. (2002). Substructure solution with SHELXD. Acta Crystallogr *D58*, 1772-1779.

Shemer, R., Meimoun, A., Holtzman, T., and Kornitzer, D. (2002). Regulation of the transcription factor Gcn4 by Pho85 cyclin PCL5. Mol Cell Biol *22*, 5395-5404.

Tan, Y. S., Morcos, P. A., and Cannon, J. F. (2003). Pho85 phosphorylates Glc7 Protein phosphatase regulator Glc8 *in vivo*. J Biol Chem *278*, 147-153.

Tarricone, C., Dhavan, R., Peng, J., Areces, L. B., Tsai, L. H., and Musacchio, A. (2001). Structure and regulation of the CDK5-p25(nck5a) complex. Mol Cell *8*, 657-669.

Terwilliger, T. C., and Berendzen, J. (1999). Automated MAD and MIR structure solution. Acta Crystallogr *D55*, 849-861.

Weeks, C. M., and Miller, R. (1999). The design and implementation of SnB version 2.0. J Appl Crystallogr *32*, 120-124.

Wilson, W. A., Mahrenholz, A. M., and Roach, P. J. (1999). Substrate targeting of the yeast cyclin-dependent kinase Pho85p by the cyclin Pcl10p. Mol Cell Biol *19*, 7020-7030.